https://doi.org/10.1093/plcell/koab272 THE PLANT CELL 2021: 00: 1–14

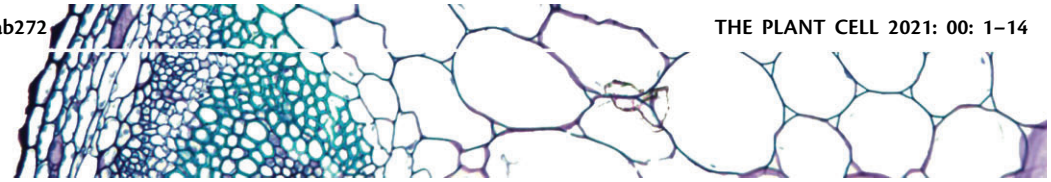

Research Article

A novel amphiphilic motif at the C-terminus of FtsZ1 facilitates chloroplast division

Xiaomin Liu [1,2] Jinjie An [1] Lulu Wang [1] Qingqing Sun [1] Chuanjing An,[3] Bibo Wu [1] Conghao Hong [1] Xiaoya Wang [3] Suwei Dong [3] Junhua Guo [4] Yue Feng [4] and Hongbo Gao [1,2,*,†]

1 National Engineering Laboratory for Tree Breeding, College of Biological Sciences and Biotechnology, Beijing Forestry University, Beijing 100083, China
2 Beijing Advanced Innovation Center for Tree Breeding by Molecular Design, Beijing Forestry University, Beijing 100083, China
3 Department of Chemical Biology, State Key Laboratory of Natural and Biomimetic Drugs, School of Pharmaceutical Sciences, Peking University, Beijing 100191, China
4 College of Life Science and Technology, Beijing Advanced Innovation Center for Soft Matter Science and Engineering, Beijing University of Chemical Technology, Beijing 100029, China

*Author for correspondence: gaohongbo@bjfu.edu.cn
†Senior author.

H.G. and X.L. conceived the project; H.G., X.L., S.D., and Y.F. designed the experiments and prepared the manuscript; X.L., J.A., L.W., Q.S., C.A., B.W., C.H., X.W., and J.G. performed the experiments. All authors read and approved the final manuscript.
The author responsible for distribution of materials integral to the findings presented in this article in accordance with the policy described in the Instructions for Authors (https://academic.oup.com/plcell) is: Hongbo Gao (gaohongbo@bjfu.edu.cn).

Abstract

In bacteria and chloroplasts, the GTPase filamentous temperature-sensitive Z (FtsZ) is essential for division and polymerizes to form rings that mark the division site. Plants contain two FtsZ subfamilies (FtsZ1 and FtsZ2) with different assembly dynamics. FtsZ1 lacks the C-terminal domain of a typical FtsZ protein. Here, we show that the conserved short motif FtsZ1 Carboxyl-terminus (Z1C) (consisting of the amino acids RRLFF) with weak membrane-binding activity is present at the C-terminus of FtsZ1 in angiosperms. For a polymer-forming protein such as FtsZ, this activity is strong enough for membrane tethering. *Arabidopsis thaliana* plants with mutated Z1C motifs contained heterogeneously sized chloroplasts and parallel FtsZ rings or long FtsZ filaments, suggesting that the Z1C motif plays an important role in regulating FtsZ ring dynamics. Our findings uncover a type of amphiphilic beta-strand motif with weak membrane-binding activity and point to the importance of this motif for the dynamic regulation of protein complex formation.

Introduction

Chloroplasts are plant-specific organelles that evolved from endosymbiotic cyanobacteria and, like their cyanobacterial precursors, chloroplasts divide by binary fission (Osteryoung and Nunnari, 2003). During the division process, a division protein complex forms a ring in the middle of the cell or organelle. The ring then constricts until two daughter cells or organelles form. Several important cell division proteins from cyanobacteria, such as filamentous temperature-sensitive Z (FtsZ) (Osteryoung and Vierling, 1995; Osteryoung et al., 1998), Filamentation 2 (Ftn2) (Vitha et al., 2003), Minicell D (MinD) (Colletti et al., 2000), and MinE (Itoh et al., 2001), were inherited by chloroplasts and function as

Received September 07, 2021. Accepted October 29, 2021. Advance access publication November 10, 2021

chloroplast division proteins. Several other chloroplast division proteins, such as ACCUMULATION AND REPLICATION OF CHLOROPLASTS5 (ARC5) (Gao et al., 2003), PLASTID DIVISION1 (PDV1) (Miyagishima et al., 2006), PDV2, and MULTIPLE CHLOROPHAST DIVISION SITE1 (Nakanishi et al., 2009), are only found in plants. Therefore, the division apparatus has changed as chloroplasts evolved from cyanobacteria during plant evolution.

FtsZ is an important division protein that is conserved in almost all bacteria and plants (Osteryoung and Nunnari, 2003; Stokes and Osteryoung, 2003). This GTPase polymerizes and forms a ring in the middle of bacterial cells or chloroplasts (Vitha et al., 2001; Errington et al., 2003). The FtsZ ring provides a scaffold for the assembly of the division apparatus (Errington et al., 2003; Osteryoung and Pyke, 2014; Wang et al., 2017; Chen et al., 2018; Barrows and Goley, 2020). Upon hydrolysis of GTP, FtsZ proteins in the ring undergo conformational changes, providing the force needed for the constriction of the division apparatus (Osawa et al., 2008; Allard and Cytrynbaum, 2009; Yoshida et al., 2016). FtsZ filaments or rings can also be depolymerized at nondivision sites by the Min system in bacterial cells or chloroplasts to ensure that the FtsZ ring forms properly in the middle of the cell or chloroplast, leading to equal division (de Boer et al., 1989; Colletti et al., 2000; Itoh et al., 2001; Zhang et al., 2013; Shaik et al., 2018).

Plants contain two FtsZ subfamilies, FtsZ1 and FtsZ2, whereas cyanobacteria and many other bacteria contain only one type of FtsZ (Stokes and Osteryoung, 2003). FtsZ1 and FtsZ2 do not function redundantly in plants (Osteryoung et al., 1998; Vitha et al., 2001; Chen et al., 2018). FtsZ in cyanobacteria contains a motif at its C-terminus that interacts with the transmembrane cell division protein Ftn2 (Mazouni et al., 2004). This interaction is conserved in chloroplasts as the C-terminus of FtsZ2 interacts with the plant Ftn2 homolog ARC6 (Zhang et al., 2016). Notably, FtsZ1 lacks this C-terminal motif. FtsZ1 and FtsZ2 also differ in their assembly and dynamics. FtsZ2 is more stable than FtsZ1, causing it to form long filaments in *FtsZ1* antisense transgenic plants (Vitha et al., 2001). FtsZ1 is more dynamic, causing it to form shorter filaments in *FtsZ2* antisense transgenic plants (Vitha et al., 2001). FtsZ1 and FtsZ2 undergo efficient co-polymerization to form FtsZ rings for chloroplast division (Yoshida et al., 2016).

Despite numerous studies, the divergence of FtsZ in plants and the difference between the two subfamilies are not fully understood. Such knowledge would be important for understanding the working mechanism of FtsZ in chloroplast division. In this study, we demonstrate that the C-terminus of FtsZ1 contains a conserved short motif consisting of a series of hydrophobic amino acids and basic amino acids in tandem without interruption. This motif is important for FtsZ1 function, has membrane-binding activity, and represents a previously unknown type of membrane-binding motif. Our findings suggest that the binding of FtsZ1 to the membrane is important for its role in chloroplast division.

Results

FtsZ1 contains an amphiphilic motif at its C-terminus that is conserved in angiosperms

FtsZ is highly conserved between cyanobacteria and chloroplasts (Osteryoung and Vierling, 1995; Osteryoung and McAndrew, 2001). However, phylogenetic analysis of FtsZ proteins in cyanobacteria and plants indicated that FtsZ diverged into two subfamilies during plant evolution as early as the appearance of green algae (Supplemental Figure S1; Supplemental Data Set S1).

The FtsZ domains of FtsZ1 and FtsZ2 subfamily members show only minor differences, but FtsZ1 lacks the C-terminal region of FtsZ2, which interacts with the transmembrane chloroplast division protein ACCUMULATION AND REPLICATION OF CHLOROPLASTS6 (ARC6) in the stroma side. Amino acid sequence alignment revealed that the C-termini of FtsZ1 proteins in different angiosperms contain a conserved motif with the sequence RRLFF (hereafter referred to as Z1C) (Figure 1). This motif is separated from the FtsZ domain by a nonconserved linker region of 20–30 amino acids (Figure 1A). The C-terminal sequences of FtsZ1 in gymnosperms, ferns, and bryophytes are somewhat similar to those in angiosperms; for instance, consisting of two continuous basic amino acids followed by three continuous hydrophobic amino acids. Generally, the closer the relationship of the plants, the higher the sequence similarity (Supplemental Table S1). These findings suggest that the Z1C motif at the C-terminus of FtsZ1 plays an important role in chloroplast division.

The C-terminal tail of FtsZ1 is important for the function of this protein

In a screen for chloroplast division mutants in *Arabidopsis thaliana*, we identified the *chloroplast division 201* (*cpd201*) mutant (Figure 2A). The *FtsZ1* gene in this mutant contains a mutation leading to a premature stop codon near its end (Figure 2B; Supplemental Figure S2). This mutation results in the truncation of 18 amino acids at the C-terminus of FtsZ1, including the Z1C motif. Immunoblot analysis indicated that this premature stop codon affects the size but not the protein level of FtsZ1 (Figure 2C). The chloroplasts in the *cpd201* mutant were heterogeneous in size, and some were obviously enlarged (Figure 2A). The number of chloroplasts per cell was greatly reduced in *cpd201* compared to the wild-type (Figure 2D; Supplemental Data Set S2). Transformation with the wild-type *FtsZ1* gene rescued the chloroplast division phenotype of the *cpd201* mutant, confirming that the mutant gene is *FtsZ1* (Figure 2, A, C, and D). Therefore, *cpd201* is an excellent mutant for exploring the function of the Z1C motif.

We also obtained an *FtsZ1* mutant by clustered regularly interspaced short palindromic repeats (CRISPR)-mediated gene editing (Supplemental Figure S3 and Supplemental

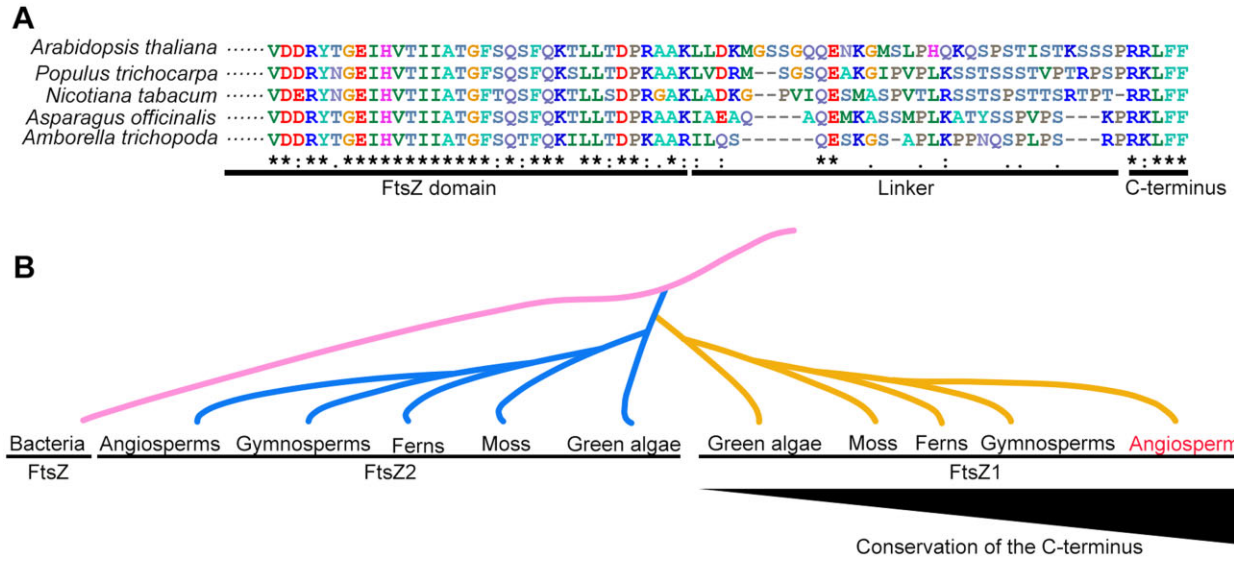

Figure 1 FtsZ1 in angiosperms contains a conserved motif at its C-terminus. A, Sequence alignment of the C-terminal regions of FtsZ1 in five angiosperms. These C-terminal regions contain a conserved motif. B, Diagram of the evolution of the C-terminal motif in FtsZ1. FtsZ1 and FtsZ2 evolved from bacterial FtsZ and started to differentiate in green algae. As plants evolved, a conserved region appeared at the C-terminus of FtsZ1 in angiosperms (highlighted in red). The pink, violet, and orange lines indicate bacterial FtsZ, plant FtsZ2, and plant FtsZ1, respectively. The black triangle indicates the increasing conservation of the C-terminus of FtsZ1.

Data Set S2). In this mutant, a single base-pair deletion near the end of *FtsZ1* resulted in a frame shift of the last 20 amino acids of FtsZ1 and a premature stop codon. The phenotype of this mutant was similar to that of *cpd201*.

To further demonstrate the importance of the Z1C motif for chloroplast division, we substituted the last five amino acids of FtsZ1 (the ZIC motif; RRLFF) with five alanines by polymerase chain reaction (PCR)-induced mutagenesis. We introduced this mutated gene (*FtsZ*^{5A}) driven by the native promoter into a null mutant of *FtsZ1*, *cpd111* (Liu et al., 2012), via transformation. We obtained many transgenic lines, as confirmed by immunoblot analysis with anti-FtsZ1 antibodies (Figure 3, A and B). Most of these plants contained levels of FtsZ1 close to that of the wild type (Figure 3B). However, the mutant phenotype was not rescued in any of these lines (Figure 3, A and C; Supplemental Data Set S2).

These results suggest that although mutations of the Z1C motif do not affect the level of FtsZ1, they do affect its function.

The C-terminal tail is important for proper FtsZ ring formation

To further explore the role of the Z1C motif in chloroplast division, we investigated the effects of this motif on the morphology of the FtsZ ring.

We performed immunofluorescence staining with FtsZ antibodies to observe the morphology of FtsZ rings in mesophyll cells. In wild-type plants, FtsZ rings were regularly distributed in the middles of chloroplasts. However, in *cpd201* and *ftsz1* CRISPR plants, the chloroplasts were enlarged, with multiple FtsZ rings or long FtsZ filaments (Figure 4; Supplemental Figure S4). In the *ftsZ1* null mutant, a similar and even stronger FtsZ ring or filament phenotype was observed (Figure 4).

We have also transformed the *FtsZ1* null mutant with constructs harboring *FtsZ1ΔC-YFP* (encoding a fusion protein lacking the last 18 amino acids of FtsZ1) and *FtsZ1-YFP*, both driven by the native *FtsZ1* promoter. *FtsZ1-YFP* rescued the chloroplast division phenotype of the *FtsZ1* mutant, and the YFP fusion protein formed rings in the centers of chloroplasts in epidermal cells of the mutant (Supplemental Figure S5). In contrast, in plants transformed with *FtsZ1ΔC-YFP*, which had similar levels of the fusion protein, the mutant phenotype was not rescued, and FtsZ rings were mostly irregular (Supplemental Figure S5). Because the native promoter was not strong, the signals in the mesophyll cells were very weak in these transgenic plants.

These data suggest that the lack of the C-terminus of FtsZ1 severely affects the proper formation of FtsZ rings and impairs their function.

It has been shown that FtsZ1 interacts with ARC3 (Zhang et al., 2013). To learn whether the C-terminal tail of FtsZ1 interacts with ARC3, we performed a yeast two-hybrid analysis and used the last 35 amino acids of FtsZ1 at the C-terminal end for the test (Supplemental Figure S6). The result indicated that this part of FtsZ1 does not interact with ARC3.

The C-terminal tail of FtsZ1 has membrane-binding activity

The Z1C motif contains two consecutive basic amino acids arginine-arginine (RR) and three hydrophobic amino acids leucine-phenylalanine-phenylalanine (LFF). Due to the

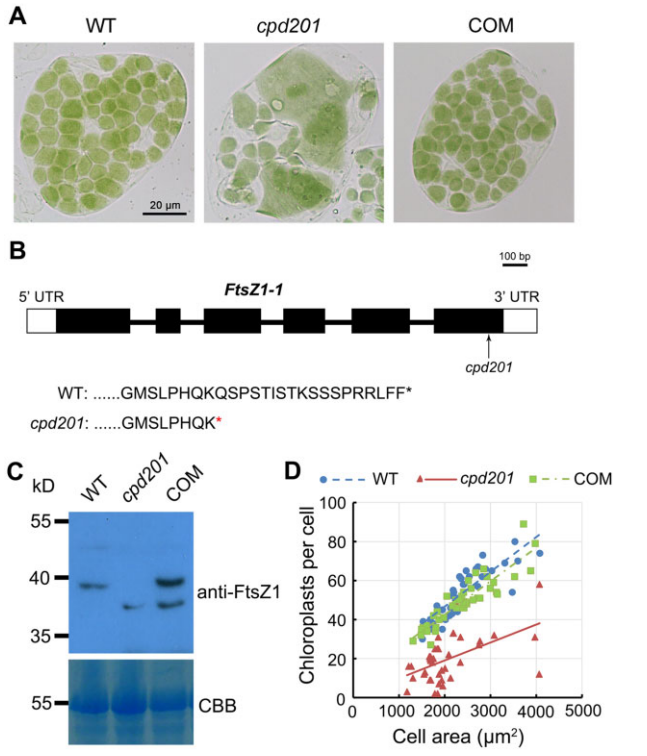

Figure 2 The C-terminus of FtsZ1 is important for its function. A, Chloroplasts in mesophyll cells from the wild-type (WT), *cpd201* mutant, and a complemented line (COM). *cpd201* is an Arabidopsis mutant of *FtsZ1* that encodes a protein that lacks the last 18 amino acids. Bar = 20 μm. The bar applies to all three images. B, Diagram of the structure of Arabidopsis *FtsZ1-1* and this gene in the *cpd201* mutant. *FtsZ1-1* contains six exons and five introns, which are represented by filled boxes and lines, respectively. The mutation site of *cpd201* is indicated by an arrow. The black and red asterisks represent the stop codon in the wild type and *cpd201* mutant, respectively. C, Immunoblot analysis of FtsZ1 probed with anti-FtsZ1 antibodies reveals a truncated form of FtsZ1 in *cpd201*. Coomassie brilliant blue (CBB) staining was used as a loading control. D, Relationship between chloroplast number and cell area in the WT, *cpd201*, and complemented line ($n > 30$ cells per sample) shown in A. The best-fit lines had slopes of 0.0178 ($R^2 = 0.7158$), 0.0092 ($R^2 = 0.2842$), and 0.0172 ($R^2 = 0.8068$) for the WT, *cpd201*, and complemented line, respectively. Three biological replicates were performed, with similar results.

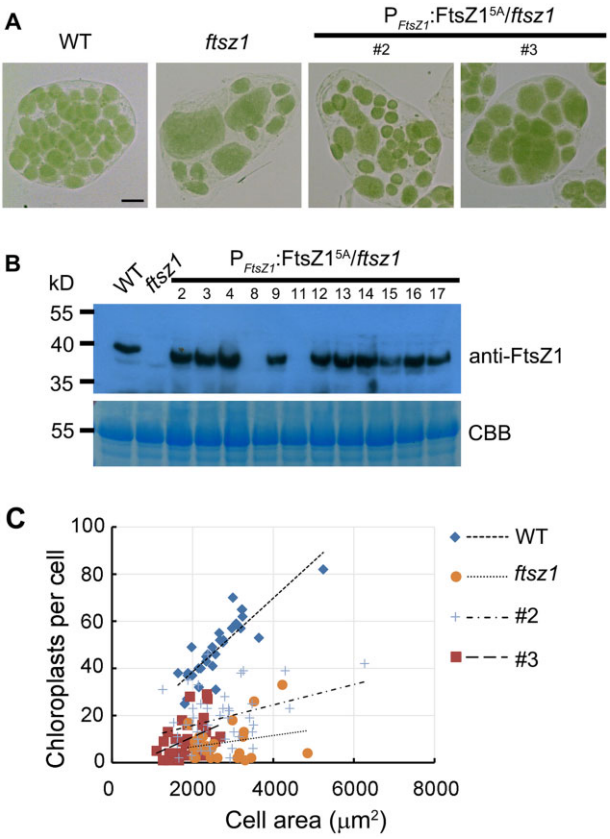

Figure 3 The last five amino acids of the C-terminus of FtsZ1 are important for its function. A, Chloroplasts in mesophyll cells from the wild type, *ftsz1*, and transgenic plant P_{FtsZ1}:FtsZ1^{5A} in the *ftsz1* background. Bar = 10 μm. All the images have the same magnification. B, Immunoblot analysis of FtsZ1 accumulation in the plants shown in (A) probed with anti-FtsZ1 antibodies. CBB staining was used as a loading control. C, Relationship between chloroplast number and cell area in wild type, *ftsz1*, and two transgenic lines ($n > 30$ cells per sample). The best-fit lines had slopes of 0.0155 ($R^2 = 0.7258$), 0.0024 ($R^2 = 0.0521$), 0.0043 ($R^2 = 0.1159$), and 0.0077 ($R^2 = 0.1636$) for the WT, *ftsz1*, and two transgenic plants, respectively. Three biological replicates were performed, with similar results.

amphiphilic nature of membrane lipids, we reasoned that this motif likely also has membrane-binding activity, even if it is weak.

To test this hypothesis, we fused the 35 C-terminal amino acids of FtsZ1 to the C-terminus of chloroplast-targeted green fluorescent protein (GFP) and transiently expressed this fusion protein in *Nicotiana benthamiana*. We then isolated chloroplasts and analyzed the membrane fraction and soluble fraction. Some GFP-Z1C35 fusion protein was present in the membrane fraction (Figure 5A). The membrane proteins YFP-PDV2 and the soluble protein Rubisco, which were used as internal controls, were primarily detected in the membrane fraction and soluble fraction, respectively. Chloroplast-targeted GFP was mostly present in the soluble fraction. When we added two C-terminal regions of FtsZ1 in tandem to the C-terminus of chloroplast-targeted GFP, the fusion protein was primarily detected in the membrane fraction (Figure 5A). A similar experiment was also done with liposomes in vitro. GFP, GFP-Z1C35, and GFP-2Z1C35 were expressed in *Escherichia coli*, purified and incubated with liposomes. A small fraction of the GFP-Z1C35 cosedimented with liposomes, and a large fraction of the GFP-2Z1C35 cosedimented with liposomes (Figure 5B). These data suggest that the C-terminal tail of FtsZ1 has membrane-binding activity and that increasing the number of this region increases the lipid-binding activity of FtsZ1 (Figure 5C).

To further analyze the membrane-binding activity of the Z1C motif, we used a previously described *E. coli* expression system (Figure 6A) in which GFP-FtsZ2-1 was expressed in *E. coli* cells (Irieda and Shiomi, 2017). In this system, GFP-FtsZ2-1 polymerized and formed long filaments in the cytosol. When a membrane-binding motif (the amphiphilic helix from the tail of EcMinD) (Szeto et al., 2002) was added to

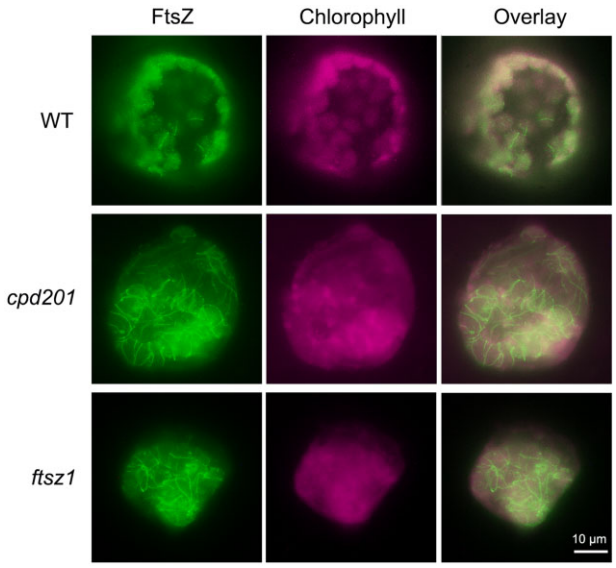

Figure 4 The C-terminal region of FtsZ1 is important for the proper formation of FtsZ rings. Immunofluorescence staining of FtsZ in wild type, *cpd201*, and *ftsz1* plants. Antibodies against full-length FtsZ2-1 and a conventional fluorescence microscope were used. The background green fluorescence is from chlorophyll. All the images have the same magnification. Bar = 10 μm. The bar refers to all images shown here.

the C-terminus of GFP-FtsZ2-1, this protein formed spiral-shaped structures, which probably were caused by membrane binding. When we added the last 35 amino acids of FtsZ1 to the C-terminus of GFP-FtsZ2-1, it also formed spiral-shaped structures (Figure 6A), suggesting that this sequence also has membrane-binding activity. When we mutated the Z1C motif of this sequence (RRLFF) into five alanines, the fusion protein simply formed long filaments (Figure 6A), suggesting that the membrane-binding activity of the fusion protein is lost.

To further pinpoint the membrane-binding sequence at the C-terminus of FtsZ1, we fused the last 10 amino acids of FtsZ1 to the C-terminus of GFP-FtsZ2-1. The fusion protein still formed spiral-shaped structures (Figure 6B), suggesting that this sequence retained its membrane-binding activity. We then mutated the "RR" in Z1C to "AA" or the "LFF" in Z1C to "AAA" and examined their effects. Both mutations abolished the membrane-binding activity of FtsZ2-1, as FtsZ2-1 only formed long filaments (Figure 6B), suggesting that both of these sequences are essential for the lipid-binding activity of this protein.

We then added an "R" after "RR" and an "L" before "LFF", changing the sequence from "RRLFF" to "RRRLLFF". FtsZ2-1 with this sequence at its C-terminus formed more condensed spirals than the other proteins (Figure 6B; Supplemental Figure S7 and Supplemental Data Set S2), suggesting that the membrane-binding activity was enhanced. However, when the two added amino acids were "AA", that is, the added sequence was "RRAALFF," FtsZ2-1 failed to form spirals, instead only forming long filaments (Figure 6B). These findings suggest that interrupting the continuity of the basic amino acids and the hydrophobic amino acids that follow abolished the membrane-binding activity of the Z1C motif.

Co-expression of GFP-FtsZ2-1 with FtsZ1 changed the pattern of GFP-FtsZ2-1 from long straight filaments into spiral-shaped filaments (Figure 6C). However, when the last five amino acids of FtsZ1 were mutated to five alanines, this effect was lost (Figure 6C). These results suggest that FtsZ1 can bring the FtsZ2/FtsZ1 co-polymers into the membrane and that the last five amino acids of FtsZ1 are essential for this function.

FtsZ proteins with a GFP tag were also transiently expressed in *N. benthamiana* leaves to study the morphology of FtsZ filaments (Figure 7). FtsZ2-1-YFP itself formed straight filaments in the stroma of chloroplasts (Figure 7; Supplemental Figure S8). GFP-FtsZ1 with the transit peptide of FtsZ1 at the N-terminus was targeted to chloroplasts but could not form any discernable filaments. FtsZ1-YFP formed aggregates in chloroplasts. However, when GFP-FtsZ1 or FtsZ1-YFP was co-expressed with FtsZ2-1, ring-shaped filaments were formed in chloroplasts. These filaments should be co-polymers of FtsZ1 and FtsZ2-1. In contrast to the straight shape of FtsZ2-1-YFP filaments, these filaments are ring-shaped, and appear to be associated with the chloroplast envelope (Figure 7; Supplemental Figure S9), a situation similar to those in bacterial cells (Figure 6).

We also tried to transiently express GFP-FTSZ1ΔC in *N. benthamiana* leaves. However, the signal was not visible. An immunoblot assay showed that the protein level was very low in comparison with the wild-type. Reverse transcription-quantitative PCR analysis showed that the gene expression level is similar to that of the wild-type. Therefore, GFP-FTSZ1ΔC is unstable in a *N. benthamiana* transient expression system and cannot be used for this analysis.

Characterization of the chemical structure of the C-terminal tail of FtsZ1

To characterize the potential conformation of the C-terminal tail of FtsZ1, the extreme C-terminal 19 amino acids of FtsZ1 (C19) and two mutants ($C19^{+RL}$ and $C19^{+AA}$) with extra amino acid residues were synthesized, and then analyzed by circular dichroism spectroscopy. After being incubated with small unilamellar vesicles (SUVs) (Figure 8A), the wild-type C19 exhibited a significantly changed CD spectrum. In contrast, the CD spectrums for $C19^{+RL}$ and $C19^{+AA}$ did not show obvious differences before and after incubation with SUVs, respectively. These data suggest that the interaction with the membrane might induce a conformational change of the C-terminal end of FtsZ1. The $C10^{+RL}$ mutant has a slightly stronger membrane-binding activity in *E. coli* cells than the wild-type (Figure 6; Supplemental Figure S7). However, the structure of $C19^{+RL}$ was not changed substantially after the membrane incubation. This could be because the binding of $C19^{+RL}$ to SUVs does not require a substantial change of the structure.

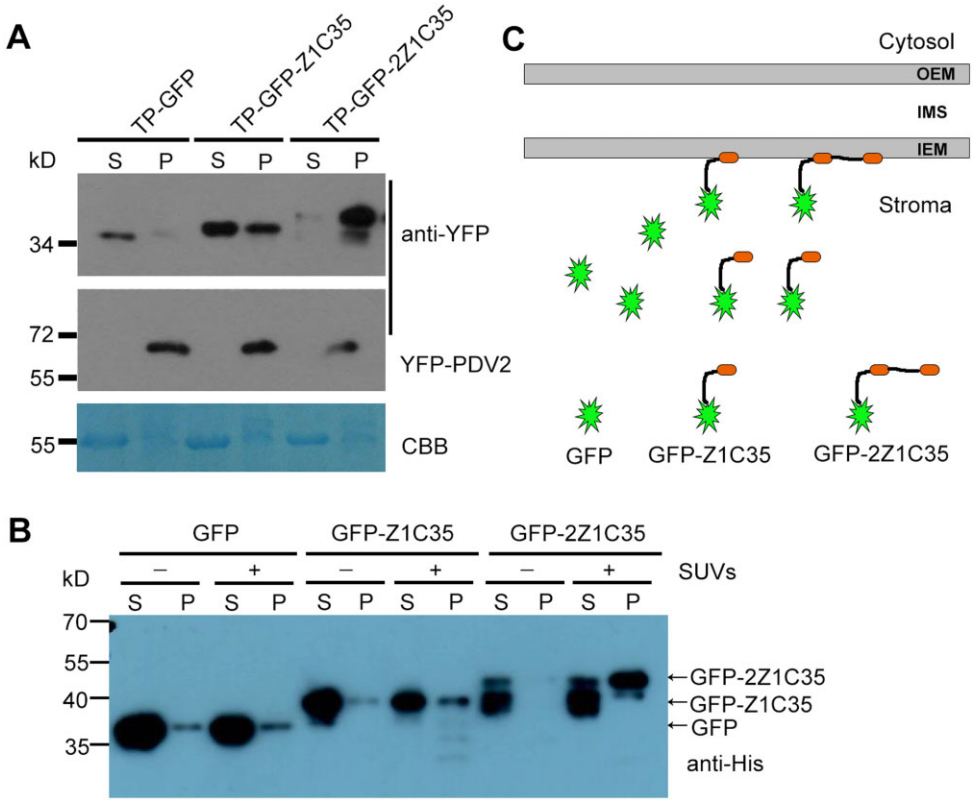

Figure 5 The C-terminal region of FtsZ1 has membrane-binding activity in chloroplasts. A, Immunoblot assay. One or two FtsZ1 C-terminal regions (35 amino acids) were fused with chloroplast-targeted GFP. These constructs were transiently expressed in *N. benthamiana* leaves. Proteins of isolated chloroplasts were separated into soluble and pellet fractions. The membrane protein YFP-PDV2 and the soluble protein Rubisco were used as controls. Both GFP and YFP were detected with YFP antibodies, and Rubisco was detected by CBB staining. B, Liposome co-sedimentation assay of GFP, GFP-Z1C35, and GFP-2Z1C35. The proteins were incubated with (+) liposomes (SUVs) or without (–) liposomes. Supernatant (S) and pellet (P) were separated by centrifugation and resolved by SDS–PAGE. Anti-His antibodies were used for the immunoblot assay. Purified GFP-2Z1C35 protein was partially degraded. C, A diagram summarizing the results is shown in (A) and (B). GFP fused with one or two Z1C35 fragments are able to bind to the membrane.

The secondary structures in these three peptide analogs were also determined. An analysis using J-1500 Spectropolarimeter (Figure 8B; Sreerama and Woody, 2000) revealed that 63.30%–79.80% of the secondary structures in these analogs consisted of beta strands. Random coils also account for a large part of the analogs, ranging from 19.70% to 23.65%, whereas helix and turns only account for a very small part. Incubation of SUVs only caused minor changes in the constitutions of the structures in these peptides. The C-terminal end of MinD in *E. coli* can form an amphiphilic helix and bind to the membrane (Szeto et al., 2002; Figure 8C). Therefore, a helical wheel model was also applied to the last 10 or 12 amino acids of these three peptides (Figure 8C). Unlike that of $EcMinD^{261–270}$, none of these three peptides could form an amphiphilic helix. Actually, upon SUV incubation, the proportions of helix were reduced and those of beta-strands were increased in these peptides (Figure 8B). Therefore, it is highly likely that the last five amino acids of FtsZ1, which are the key part for membrane binding, may have a beta-strand structure. This sequence may have a relatively extended form, and the extent and variation of the extension may play an important role in membrane binding and regulation of chloroplast division.

Discussion

In this study, we demonstrated that the C-terminus of FtsZ1 contains a novel motif that is conserved in angiosperms. The C-terminus of FtsZ in cyanobacteria or FtsZ2 in plants interacts with the transmembrane protein Ftn2 (or its homolog ARC6) and is anchored to the membrane at the division site (Mazouni et al., 2004; Zhang et al., 2016). Similarly, in *E. coli*, the C-terminus of FtsZ interacts with the transmembrane protein ZipA and membrane anchoring protein FtsA to ensure its membrane localization and proper functioning (Hale and de Boer, 1997; Din et al., 1998). Compared to these protein-interacting motifs, the FtsZ1 Carboxyl-terminus (Z1C) motif is much shorter (Figure 1), containing only five amino acids. Nonetheless, this motif is important for the proper functioning of the protein (Figures 2–4), it binds to the membrane (Figures 5, 6, and 8) and helps

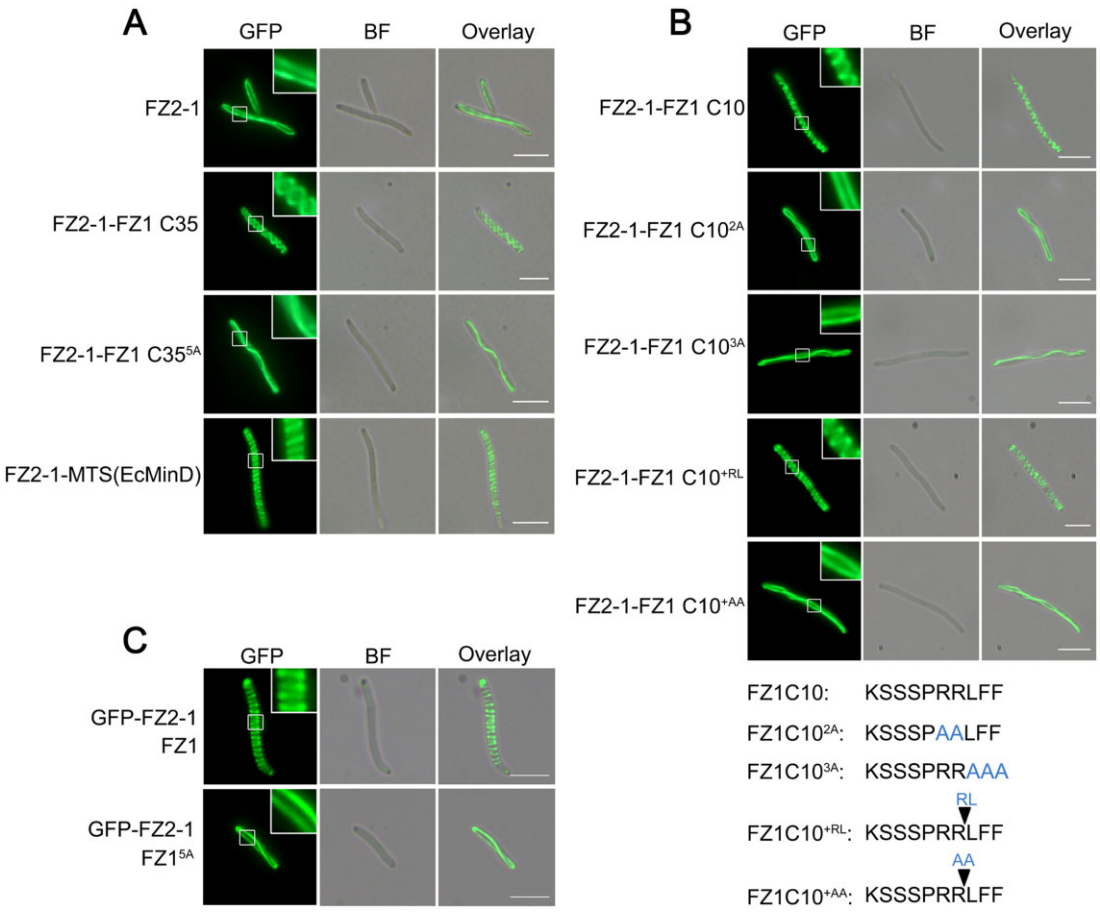

Figure 6 The C-terminal region of FtsZ1 has membrane-binding activity in *E. coli*. The effects of the C-terminal region of FtsZ1 and various mutants on the membrane binding of GFP-FtsZ2-1 in *E. coli*. In this assay, fusion proteins that polymerize and bind to the membrane form helices in the *E. coli* cells. The insets in the upper-right corners of the images show three times magnified views of the regions highlighted by white boxes. BF, bright field; Bar = 5 μm. A, The last five amino acids of FtsZ1 are essential for its membrane binding. FtsZ2-1-FZ1 C35, the last 35 amino acids of FtsZ1 fused to the C-terminus of FtsZ2-1; $C35^{5A}$, the last five amino acids of FtsZ1 were substituted with five alanines; MTS(EcMinD), membrane-tethering sequence of MinD in *E. coli*. B, A detailed analysis of the C-terminus of FtsZ1 with various mutations. FZ1 C10, the last 10 amino acids of FtsZ1. A diagram of the mutations in various mutants, such as substitutions and insertions, is shown below the images. Blue font indicates the mutations. C, Co-expression of GFP-FtsZ2-1 and FtsZ1 or $FtsZ1^{5A}$ in *E. coli*. In $FtsZ1^{5A}$, the last five amino acids of FtsZ1 were changed to five alanines.

FtsZ1 bring FtsZ2 filaments to the chloroplast envelope (Figure 7).

Interestingly, FtsZ proteins in plants evolved into two subfamilies (Stokes and Osteryoung, 2003). Furthermore, FtsZ diverged into two subfamilies in red algae (Miyagishima et al., 2004), FtsZA and FtsZB, with different assembly dynamics (Chen et al., 2017). FtsZ proteins polymerize via their FtsZ domains (Olson et al., 2010). The sequences of the FtsZ domains in FtsZ1 and FtsZ2 are generally conserved, but with some differences. FtsZ2 can polymerize into rings and filaments (Yoshida et al., 2016), whereas FtsZ1 is less able to polymerize (Vitha et al., 2001). FtsZ1 is more dynamic, but it can co-polymerize with FtsZ2 (Yoshida et al., 2016). This is likely important for the dynamics of FtsZ rings, that is, depolymerization at nondivision sites and constriction at the division site. In *E. coli*, the membrane protein MinD, which harbors an amphiphilic protein helix at its C-terminus (Szeto et al., 2002), recruits MinC to the membrane (Hu and Lutkenhaus, 1999). MinC interacts with FtsZ and prevents it from forming FtsZ rings at nondivision sites (Hu et al., 1999). Without MinD, MinC localizes to the cytosol and its function cannot be fulfilled. During the evolution of plants, MinC was lost, and its function was likely replaced by ARC3 (Zhang et al., 2013). ARC3, a FtsZ-like protein, interacts with other membrane proteins such as MinD and PARC6 to prevent the formation of FtsZ rings at nondivision sites (Maple et al., 2007; Glynn et al., 2009; Zhang et al., 2009; Shaik et al., 2018). In our *ftsZ* mutants lacking the C-terminus, chloroplasts were heterogeneous in size, and FtsZ proteins formed multiple parallel rings or long filaments (Figure 4). These phenotypes are indicative of a defective Min system. FtsZ filaments in those mutants are anchored to membrane through the direct interaction between FtsZ2 and the transmembrane protein ARC6 (Schmitz et al., 2009). This makes the filaments more resistant to the Min system, which hampers chloroplast division. In the wild-type, the membrane

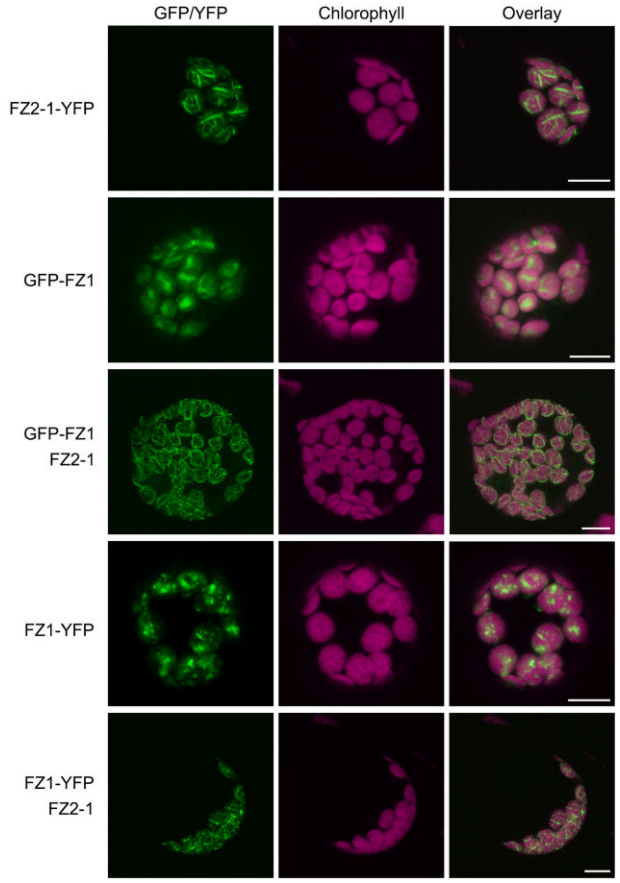

Figure 7 FtsZ1 brings FtsZ2 filaments to the chloroplast envelope. FtsZ proteins with YFP or GFP tags were transiently expressed in *N. benthamiana* leaves. Proteins expressed are indicated on the left. GFP-FtsZ1 has the chloroplast transit peptide of FtsZ1 at the N-terminus. To get a clear view, protoplasts were isolated for observation. Some confocal Z-stack slices of the copolymers are shown in Supplemental Figures S8 and S9. Bar = 10 μm.

interaction of FtsZ1–FtsZ2 co-polymers through the Z1C motif of FtsZ1 (Figure 9) facilitates Min system activity on the FtsZ filaments at non-division sites and is important for the proper division of chloroplasts.

In our *N. benthamiana* transient expression system, GFP-FtsZ1 did not form filaments and FtsZ1-YFP tended to aggregate in chloroplasts (Figure 7). In FtsZ2-1 antisense transgenic Arabidopsis plants, endogenous FtsZ1 is mainly in short filaments and foci (Vitha et al., 2001), which is similar to our results. These data are different from the results in *Schizosaccharomyces pombe* (TerBush et al., 2016), which showed that FtsZ1FL-mVenus can form long filaments. This probably is because in their system, FtsZ1 proteins were expressed in the cytosol of eukaryotic cells, which have a more complicated protein folding system than chloroplasts and could facilitate protein polymerization and filament formation. Moreover, FtsZ filaments in chloroplasts are regulated by Min system and some other different factors.

There are many types of protein–membrane interactions. For example, transmembrane proteins containing transmembrane helixes or strands are tightly imbedded in the membrane. Some other membrane proteins associate with the membrane in more dynamic ways. For example, lipid molecules can attach to membrane proteins, causing these proteins to target the membrane (Resh, 2016). Membrane proteins can also bind to the head groups of phospholipids and localize to membranes (Manna et al., 2008; Potocký et al., 2014; Simon et al., 2016). In the Min system of *E. coli*, the C-terminus of MinD contains an amphiphilic helix that helps tether the protein to the membrane (Szeto et al., 2002). These types of membrane proteins interact with the membrane in a manner that can be regulated or can easily move in the membrane.

The way in which a membrane protein interacts with the membrane is related to its function. The C-terminus of FtsZ1 contains a special beta-strand type membrane-binding motif (Figure 8) comprising several basic amino acids in a row and several continuous hydrophobic amino acids in a row, without interruption (Figure 9). The membrane-binding activity of a single motif of this type is relatively weak, even weaker than that of the C-terminal motif of EcMinD (Figure 6; Supplemental Figure 7). As demonstrated in this study, when a protein complex contains multiple motifs of this type, its membrane-binding activity is much stronger and it can attach to the membrane well (Figures 5, 6, 8, and 9). This weak binding activity is necessary, as it probably makes FtsZ filaments comprising FtsZ1 and FtsZ2 co-polymers prone to the regulation of the Min system on the inner envelope at nondivision sites (Figure 4). The lipid-binding motif at the C-terminus of FtsZ1 is small and simple, suggesting that this type of motif would evolve relatively easily in other proteins if it had an advantage. The weak lipid-binding activity of this beta-strand type motif might be required for a protein to function in a dynamic manner.

Materials and methods

Plant materials

Arabidopsis thaliana ecotype Col-0 was used in this study. *cpd201*, a chloroplast division mutant with a mutation in *FtsZ1* gene, was obtained from the M2 generation of an ethyl methane sulfonate mutagenized population of Col-0 background. Plants were grown in soil at 22°C with a photoperiod of 16-h light/8-h dark and a light intensity of 80–100 μmol m^{-2} s^{-1} from Philips Essential TL5 28w/865 fluorescent lamps (Philips Lighting UK, Guildford, UK). Leaves of approximately 40-day-old *N. benthamiana* plants were used for Agrobacterium-mediated transient expression.

To generate CRISPR mutants of *FtsZ1*, a specific site in *FtsZ1* was selected as the target of Cas9 with the website CRISPRscan (http://www.crisprscan.org/) and CAS-OFFinder (http://www.rgenome.net/cas-offinder/). Vectors were constructed and mutants were identified as described (Xing et al., 2014; Wang et al., 2015). The PCR fragment was amplified using primer Oligo-1-F and Oligo-1-R (Supplemental Table S2). The product was cloned into the pHEE401E vector with BsaI and T4 Ligase. Wild-type plants of Arabidopsis Col-0 were used for transformation via the floral dipping

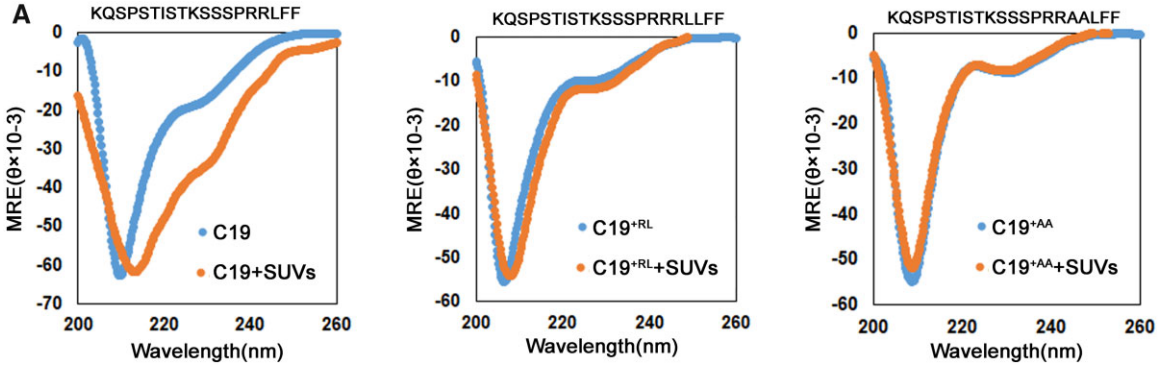

B

	C19	C19 +SUVs	$C19^{+RL}$	$C19^{+RL}$ +SUVs	$C19^{+AA}$	$C19^{+AA}$ +SUVs
Helix	6.10%	3.10%	3.00%	0.50%	2.80%	1.90%
Beta	63.30%	66.30%	72.30%	79.80%	72.10%	75.20%
Turn	7.00%	2.95%	2.80%	0.00%	1.60%	0.90%
Random	23.60%	27.65%	21.90%	19.70%	23.50%	22.00%
Total	100%	100%	100%	100%	100%	100%

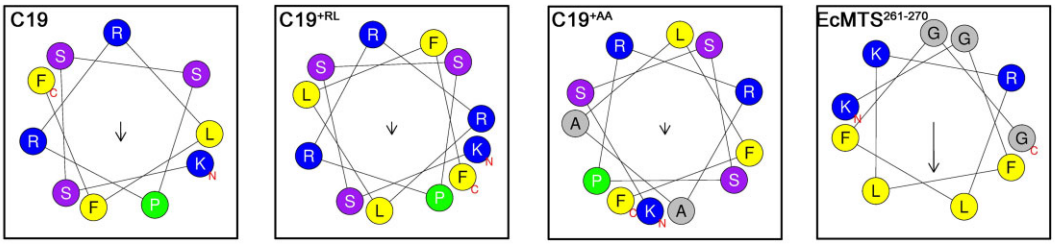

Figure 8 Secondary structure analysis of the C-terminal end of FtsZ1. A, CD spectrum of peptide analogs of the extreme C-terminal 19 amino acids of FtsZ1 (C19) and the two insertion mutants $C19^{+RL}$ and $C19^{+AA}$ as shown in Figure 6B, with or without SUVs. Peptide sequences are given above the spectra. MRE is the mean residue ellipticity in units of degrees cm2 dmol-1. B, Determination of the secondary structure constitutions in peptides analyzed in (A) using the protein secondary structure analysis tool of J-1500. C, Helical wheel prediction (https://heliquest.ipmc.cnrs.fr/) of C10, $C10^{+RL}$, and $C10^{+AA}$ peptides of FtsZ1 as shown in Figure 6B. Only 10 or 12 amino acids were used in the analysis.

method (Clough and Bent, 1998). T_1 seeds were screened on 1/2 murashige and skoog (MS) plates containing 20 mg/L hygromycin and 10 mg/L carbenicillin. Genomic DNA was extracted from T_1 transgenic plants, amplified by PCR, and sequenced for mutant identification. Homozygous mutants were obtained from T_3 plants.

Bioinformatics analysis

Protein sequences of FtsZ1 and FtsZ2-1 in *A. thaliana* and their homologous sequences in other species were identified by BLAST at National Center for Biotechnology Information (https://blast.ncbi.nlm.nih.gov/Blast.cgi) and downloaded. Sequence alignment of Arabidopsis FtsZ1 and its homologs, and analysis of the sequence similarity of the C-terminus of FtsZ1proteins were carried out using BioEdit version 7.2.5 software (https://bioedit.software.informer.com/). Maximum likelihood phylogenetic analysis of FtsZ proteins was carried out using MEGA7 (https://megasoftware.net/). Branching confidence was estimated using 1,000 bootstrap replicates.

Chloroplast phenotype analysis

Leaf fixation and chloroplast phenotype analysis were conducted as previously reported (Gao et al., 2013; Chang et al., 2015). Arabidopsis leaves from soil-grown 40-day-old plants were immersed in 3.5% glutaraldehyde and fixed for 1 h in darkness. Images of chloroplasts were taken with an Olympus CX21 microscope (Olympus, Tokyo, Japan) equipped with a USB 2.0 digital camera (Changheng, Beijing, China). Statistical analysis of chloroplast phenotypes was performed as described previously (Supplemental Data Set S2; Gao et al., 2013).

Fluorescence microscopy

To detect yellow fluorescent protein (YFP), green fluorescent protein (GFP) and chlorophyll fluorescence from leaf tissues, a TCS SP8 confocal laser scanning microscope (Leica Microsystems, Wetzlar, Germany) equipped with both photomultiplier tube (PMT) and hybrid detector (HyD) was used. The signal from chlorophyll of chloroplasts was collected by the PMT detector and the signal from YFP or GFP

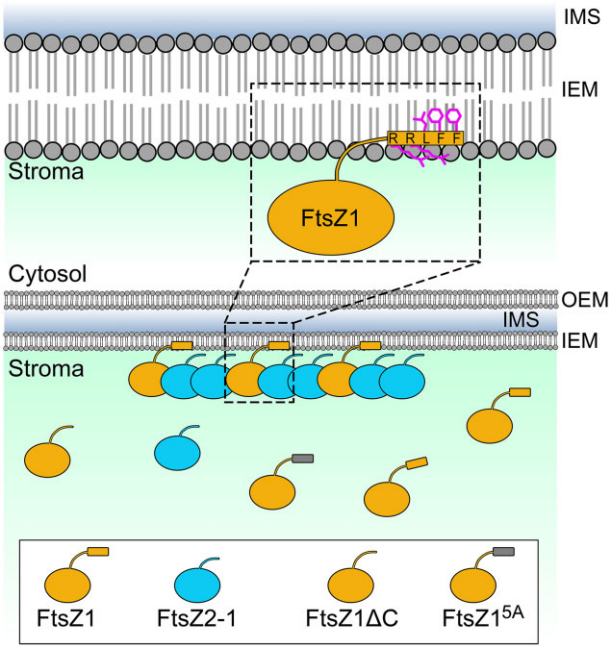

Figure 9 Working model of the structure and activity of the C-terminus of FtsZ1. The Z1C motif helps the FtsZ2/FtsZ1 copolymer bind to the chloroplast inner envelope. Upper half of the diagram: The hydrophobic amino acids "LFF" at the C-terminus bind to the inside of the membrane, while the basic amino acids "RR" bind to the hydrophilic surface of the membrane. Lower half of the diagram: the Z1C motif helps FtsZ filaments bind to the inner envelope membrane of the chloroplast. When only one FtsZ1 protein is present, its binding ability is not very strong. When multiple FtsZ1 proteins are present in FtsZ1 and FtsZ2 copolymers, the Z1C motif helps FtsZ filaments bind to the membrane. When the C-terminus of FtsZ1 is removed (FtsZ1△C) or the last five amino acids at its C-terminus mutated (FtsZ1^{5A}), FtsZ1 loses its ability to bind to the membrane. OEM, outer envelope membrane; IMS, inter-membrane space; IEM, inner envelope membrane.

was collected by the HyD. The numerical aperture of the 63× oil immersion objective was 1.4. The excitation wavelength of YFP or GFP was 489 nm and the emission was 525 ± 20 nm. Chlorophyll was excited using 489 nm lasers, and emission was collected through 668 ± 20 nm filters. Pinhole size was at 1.0 airy units for all experiments. The *E. coli* cells were imaged at 100× magnification using a fluorescence microscope (NE910, Nexcope, Ningbo, China) equipped with a digital camera (E31SPM, Hangzhou Touptek Photonics Co., Ltd.). The numerical aperture of the oil immersion 100× objective was 1.3. The excitation wavelength of GFP was 460–490 nm and the emission spectra were collected from 510 to 550 nm. Fluorescence images were processed with Adobe Photoshop CC software (https://www.adobe.com/products/photoshop.html) for contrast/brightness adjustments and cropping.

Antibodies and immuno analysis

Full-length FtsZ1 and FtsZ2-1 and a 15 amino acid–peptide of FtsZ1 (the 201th residue to the 215th residue; Stokes et al., 2000) were used to generate antibodies in rabbits.

For immunoblot analysis, proteins were extracted from leaves of 40-day-old Arabidopsis plants. Protein samples were separated on sodium dodecyl sulphate–polyacrylamide gel electrophoresis (SDS–PAGE) gels and transferred to polyvinylidene fluoride (PVDF) membrane (Bio-Rad, Hercules, CA, USA). Blots were probed with purified anti-FtsZ1 peptide antibodies with a dilution of 1:2000 in TBST (50 mM Tris, 150 mM NaCl, and 0.05% Tween-20, pH 7.5) containing 3% milk. The ECL Western Blot kit (Beijing ComWin Biotech Company, China) was used to detect the immunoreactive protein bands. The peptide antibodies were used for the experiments represented in Figures 2, 3 and Supplemental Figure S3. Antibodies against full-length FtsZ1 were used in Supplemental Figure S5.

Immunofluorescence staining of FtsZ proteins in chloroplasts was carried out as previously described (Li et al., 2016). Antibodies against full-length FtsZ2-1 were used.

Chloroplast isolation and fractionation

Agrobacteria containing various constructs were infiltrated into leaves of 40-day-old *N. benthamiana* plants. Forty-eight hours later, intact chloroplasts were isolated using a Percoll gradient, lysed by freeze–thaw cycles, and further separated into membrane fractionation and soluble fraction as described (Chu and Li, 2011). Protein samples were resolved by SDS–PAGE and analyzed by immunoblot. The YFP antibodies are from Biodragon (Beijing, China).

Plasmid constructions for expression in plants or *E. coli*

To make a complementation construct for *cpd201*, a 2.8-kb region of FtsZ1 genomic sequence including a 0.8-kb promoter region was amplified using primers FZ1-10 and FZ1-14 (Supplemental Table S2). The DNA fragment was digested with BamHI and NcoI, and ligated into a 3302Y3 transformation vector that had been digested with the same restriction enzymes. The construct was verified by sequencing and transformed into the *cpd201* mutant by the floral dipping method. Transgenic plants were selected with 60 mg/L glufosinate in soil.

P_{FtsZ1}:FtsZ1^{5A}, P_{FtsZ1}:FtsZ1-YFP, and P_{FtsZ1}:FtsZ1△C-YFP were constructed based on the complementation construct, P_{FtsZ1}:FtsZ1. P_{FtsZ1}:FtsZ1^{5A} was amplified by PCR using primers FZ1-10 and FZ1–35. The PCR fragment and 3302Y3 vector were digested with both BamHI and NcoI and then ligated together. To obtain P_{FtsZ1}:FtsZ1-YFP, the *FtsZ1* gene was PCR amplified with primers FZ1–10 and FZ1–11, digested with BamHI and NcoI, and then ligated into the 3302Y2 vector. FtsZ1△C that lacks the last 18 amino acids at the C terminus of FtsZ1 was amplified by PCR using primer FZ1–10 and FZ1–25. The PCR fragment and 3302Y2 vector were digested with both BamHI and AatII, and then ligated together. These constructs were introduced into the *ftsz1* mutant by the floral dipping method. Transgenic plants were selected with 60 mg/L glufosinate in soil.

To analyze the membrane-binding activity of the Z1C motif, various sequences were constructed. 35S:TP-GFP was

constructed as previously (Gao et al., 2006). The fragment of TP from *AT1G03160* was amplified by PCR using primers Nco1TP and TP-Pst1. GFP was amplified using primers Pst1GFP and GFPKpn1, and Z1C35 and 2Z1C35 were amplified using primers Z1MTS-U2 and Z1MTS-MluI. These three fragments (TP, GFP, and Z1MTS or TP, GFP, and 2Z1C35) were fused together by PCR, then digested with NcoI and MluI, and ligated into the 3302Y2 vector to generate 35S:TP-GFP-Z1C35 and 35S:TP-GFP-2Z1C35. These constructs were transiently expressed in *N. benthamiana* leaves by Agrobacteria infiltration for further biochemical analysis.

To express GFP, GFP-Z1C35, and GFP-2Z1C35 in *E. coli* BL21 for protein purification, the *GFP* gene was amplified with primers Nco1GFP and GFPHindIII, and GFP-Z1C35 and GFP-2Z1C35 were amplified with primers Nco1GFP and Z1MTS-D. These fragments were cloned into pET-30a between the NcoI and HindIII sites.

To construct GFP-FtsZ2-1, the coding sequence of FtsZ2-1 (without the transit peptide, i.e. 48 amino acids at the N terminus) was amplified with primers FZ2-1–43 and FZ2-1–44, GFP was amplified with Nco1GFP and GFPEcoR1, and the two fragments were fused together by PCR and ligated into pET-28a between the NcoI and HindIII sites. "FZ1 C35" was amplified with primers Z1MTS-U3 and Z1MTS-D3, and "FZ1 C35^{5A}" was amplified with primers Z1MTS-2A-U and Z1MTS-3A-D2. These two fragments were digested with HindIII and XhoI, and then added to the coding sequence of GFP-FtsZ2-1 at the 3′-end, respectively. Coding sequences of the last 10 amino acids at the C terminus of MinD in *E. coli* were amplified using primer MinD-C-Z2, then digested with Xho1 and added to the 3′-end of GFP-FtsZ2-1. GFP-FtsZ2-1-FtsZ1C10, GFP-FtsZ2-1-FtsZ1C10^{2A}, GFP-FtsZ2-1-FtsZ1C10^{3A}, GFP-FtsZ2-1-FtsZ1C10^{+RL}, and GFP-FtsZ2-1- FtsZ1C10^{+AA} were amplified using the forward primer Nco1GFP, and reverse primers FZ1–46, FZ1–47, FZ1–48, FZ1–51, and FZ1–52, respectively, with GFP-FtsZ2-1-FZ1 C35 as template. These constructs were expressed in *E. coli* BL21 and their localizations were observed (Figure 6, A and B).

To co-express GFP-FtsZ2-1 and FtsZ1 or FtsZ1^{5A} in *E. coli* BL21, the *GFP-FtsZ2-1* fusion was amplified with primers Sac1GFP and FZ2-1–48 and inserted into the first gene expression cassette of the pETDuet-1 vector, and then the *FtsZ1* or *FtsZ1^{5A}* gene was amplified with FZ1–54, FZ1–55, or FZ1–56, respectively, and inserted into the second gene expression cassette.

To generate 35S:FtsZ2-1-YFP, the *FtsZ2-1* gene was amplified using primers FZ2-1–38 and FZ2-1–45, then ligated into the 3302Y4 vector between EcoRI and HindIII. To generate 35S:TP-GFP-FtsZ1, TP-GFP was amplified using primers FZ1–29 and GFPKpn1 with TP-GFP-Z1C35 as template, while the genomic DNA fragment of *FtsZ1* was amplified using primers FZ1–28 and FZ1–14. Then TP-GFP and FtsZ1 were ligated simultaneously into the 3302Y4 vector between EcoRI and NcoI. To generate 35S:FtsZ2-1, the coding region of the *FtsZ2-1* gene was amplified by PCR using primers FZ2-1-5 and FZ2-1-8, digested with NcoI, and ligated into the 3302Y2 vector between the NcoI and PmlI cutting sites. These constructs were transiently expressed in *N. benthamiana* leaves by Agrobacteria infiltration.

Protein expression in *E. coli* and purification

His-tagged GFP, GFP-Z1C35, and GFP-2Z1C35 were expressed in *E. coli* BL21 strains. Bacterial cells expressing these proteins were grown overnight in 5-mL LB medium at 37°C and transferred to 500-mL LB medium. The cultures were grown until the optical density at 600 nm (OD_{600}) reached ~0.8 and were then cold-shocked for 10 min in an ice bath. Isopropyl-β-D-1-thiogalactopyranoside was added to a final concentration of 0.5 mM. The cultures were grown at 20°C for 20–24 h. The cells were harvested by centrifugation.

Cell pellets were resuspended in wash buffer (50 mM NaH_2PO_4, 300 mM NaCl, 20 mM imidazole) with 0.1 mg/mL phenylmethylsulfonyl fluoride (PMSF) at 4°C. Since PMSF is unstable in an aqueous solution, it was added every 30 min. Cells were ruptured by sonication. The lysates were centrifuged at 30,000*g* for 30 min at 4°C and the pellet was discarded. Soluble proteins were loaded onto the column prepacked with Ni-Agarose Resin (CoWin Biosciences, Cambridge, MA, USA). The column was then washed with two different concentrations of imidazole (20 mM, 30 mM) in wash buffer and the protein was eluted in 500-mM imidazole in wash buffer. Purified proteins were dialyzed into PBS (10-mM phosphate, 150-mM NaCl, and pH7.4) at 4°C, aliquoted, and stored at −80°C.

Liposome co-sedimentation

Liposomes were made from dioleoyl phosphatidylcholine and dipalmitoyl phosphatidylglycerol (1:1; M:M) using a rotary evaporator, vortex mixer, and filter. His-GFP, His-GFP-Z1C35, and His-GFP-2Z1C35 proteins were centrifuged at 20,000*g* for 10 min at 4°C to remove precipitate. The soluble part of the proteins was transferred to prechilled tubes and kept on ice. Then the proteins were added to liposomes or PBS buffer. The mixtures were incubated at room temperature for 1 h and centrifuged at 15,000*g* for 10 min at room temperature to separate the supernatant and pellet. The samples were resolved by SDS–PAGE. Blots were probed with a mouse monoclonal anti-His antibody (Beijing Biodragon Immunotechnologies, B1004) at a dilution of 1:3,000 in TBST (50-mM Tris, 150-mM NaCl, and 0.05% Tween-20, pH 7.5) with 3% nonfat dry milk and anti-mouse IgG secondary antibody at a dilution of 1:10,000.

Yeast two-hybrid analysis

ARC3$^{41–598}$ was amplified using primers ARC3–39 and ARC3–40 (Supplemental Tables S2), digested with EcoRI and BamHI and cloned into pGADT7 vector. FtsZ1$^{59–433}$ was amplified with primers FZ1–54 and FZ1–55, and Z1C35 was amplified with primers Z1MTS-U4 and Z1MTS-D4. These two fragments were cloned into the pGBKT7 vector between the NcoI and BamHI sites. The respective combinations of constructs were co-transformed into yeast strain

AH109. Transformed yeast cells were separately spread onto 2D synthetic dropout medium (−Leu/−Trp) and 3D selective medium (Leu/−Trp/−His) and incubated at 30°C for 3 days. To determine the intensity of protein interaction, saturated yeast cultures were diluted to 10^{-1} and 10^{-2} and then spotted onto selection medium.

Peptide synthesis and circular dichroism spectroscopy

Peptides were synthesized (0.05 mmol) with Liberty Blue Automated Microwave Peptide Synthesizer (CEM, Charlotte, NC, USA) using standard solid-phase peptide synthesis protocol. The Fmoc-amino acids, in four-fold excess, were assembled using HATU/DIEA as coupling agents. The resin-bound products were cleaved by trifluoroacetic acid and purified by preparative HPLC separation. Peptide (1 mg/mL) or Peptide/SUV (molar ratio was 1:50) samples were dissolved in PBS buffer (pH 7.4). CD spectra were measured with a J-1500 Spectropolarimeter (JASCO, Easton, MD, USA) in a 1 mm path length quartz cuvette (Hellma, New York, USA). Far-UV spectra were recorded from 200 to 260 at 25°C. To acquire the spectra, at least three scans were used for the average calculation.

Accession numbers

Sequence data from this article can be found in The Arabidopsis Information Resource (TAIR) (www.arabidopsis.org) with the following accession numbers: *FtsZ1* (At5g55280), *FtsZ2-1* (At2g36250); Supplemental Table S1 and Supplemental Data Set S1.

Supplemental data

The following materials are available in the online version of this article.

Supplemental Figure S1. A phylogenetic tree of the protein sequences of FtsZ1 and FtsZ2 in plants, and their homologs in Cyanobacteria (Supports Figure 1).

Supplemental Figure S2. Sequencing analysis of *cpd201* mutant (Supports Figure 2).

Supplemental Figure S3. Phenotype and statistical analysis of mutants obtained by CRISPR/Cas9 (Supports Figure 2).

Supplemental Figure S4. Immunofluorescence staining of FtsZ (Supports Figure 4).

Supplemental Figure S5. The C-terminal region of FtsZ1 affects the localization pattern of FtsZ1 (Supports Figure 4).

Supplemental Figure S6. The C-terminus of FtsZ1 doesn't interact with ARC3 (Supports Figure 4).

Supplemental Figure S7. Statistical analysis of the density of FtsZ spirals in Figure 6, A and B (Supports Figure 6).

Supplemental Figure S8. Confocal Z-stack slices of FtsZ2-1-YFP (Supports Figure 7).

Supplemental Figure S9. Confocal Z-stack slices of GFP-FtsZ1 + FtsZ2-1 (Supports Figure 7).

Supplemental Table S1. Sequences of Z1C-like motifs in Bryophytes, Ferns, and Gymnosperms (Supports Figure 1).

Supplemental Table S2. Primers used in this study.

Supplemental Data Set S1. Alignment of sequences used to generate the phylogeny presented in Supplemental Figure S1.

Supplemental Data Set S2. Details of the statistical analysis in Figures 2, D and 3, C and Supplemental Figures S3D and S7.

Acknowledgments

The authors thank professors Kathy Osteryoung (Michigan State University) and Tonglin Mao (China Agricultural University) for the helpful discussions and suggestions. The authors also thank professors Qi-Jun Chen (China Agricultural University) for kindly providing the vectors and strains of CRISPR/Cas9.

Funding

This work was supported by grants from the National Natural Science Foundation of China to X.L. (31501090) and H.G. (31570182, 32070696).

Conflict of interest statement. The authors declare no conflict of interests.

References

Allard JF, Cytrynbaum EN (2009) Force generation by a dynamic Z-ring in Escherichia coli cell division. Proc Natl Acad Sci USA **106:** 145–150

Barrows JM, Goley ED (2020) FtsZ dynamics in bacterial division: what, how, and why? Curr Opin Cell Biol **68:** 163–172

Chang N, Gao Y, Zhao L, Liu X, Gao H (2015) Arabidopsis FHY3/CPD45 regulates far-red light signaling and chloroplast division in parallel. Sci Rep **5:** 9612

Chen C, MacCready JS, Ducat DC, Osteryoung KW (2018) The molecular machinery of chloroplast division. Plant Physiol **176:** 138–151

Chen Y, Porter K, Osawa M, Augustus AM, Milam SL, Joshi C, Osteryoung KW, Erickson HP (2017) The chloroplast tubulin homologs FtsZA and FtsZB from the red alga Galdieria sulphuraria co-assemble into dynamic filaments. J Biol Chem **292:** 5207–5215

Chu CC, Li HM (2011) Determining the location of an Arabidopsis chloroplast protein using in vitro import followed by fractionation and alkaline extraction. Methods Mol Biol **774:** 339–350

Clough SJ, Bent AF (1998) Floral dip: a simplified method for Agrobacterium-mediated transformation of Arabidopsis thaliana. Plant J **16:** 735–743

Colletti KS, Tattersall EA, Pyke KA, Froelich JE, Stokes KD, Osteryoung KW (2000) A homologue of the bacterial cell division site-determining factor MinD mediates placement of the chloroplast division apparatus. Curr Biol **10:** 507–516

de Boer PA, Crossley RE, Rothfield LI (1989) A division inhibitor and a topological specificity factor coded for by the minicell locus determine proper placement of the division septum in E. coli. Cell **56:** 641–649

Din N, Quardokus EM, Sackett MJ, Brun YV (1998) Dominant C-terminal deletions of FtsZ that affect its ability to localize in Caulobacter and its interaction with FtsA. Mol Microbiol **27:** 1051–1063

Errington J, Daniel RA, Scheffers DJ (2003) Cytokinesis in bacteria. Microbiol Mol Biol Rev **67:** 52–65

Gao H, Sage TL, Osteryoung KW (2006) FZL, an FZO-like protein in plants, is a determinant of thylakoid and chloroplast morphology. Proc Natl Acad Sci USA **103:** 6759–6764

Gao HB, Kadirjan-Kalbach D, Froehlich JE, Osteryoung KW (2003) ARC5, a cytosolic dynamin-like protein from plants, is part of the chloroplast division machinery. Proc Natl Acad Sci USA **100:** 4328–4333

Gao Y, Liu H, An C, Shi Y, Liu X, Yuan W, Zhang B, Yang J, Yu C, Gao H (2013) Arabidopsis FRS4/CPD25 and FHY3/CPD45 work cooperatively to promote the expression of the chloroplast division gene ARC5 and chloroplast division. Plant J **75:** 795–807

Glynn JM, Yang Y, Vitha S, Schmitz AJ, Hemmes M, Miyagishima SY, Osteryoung KW (2009) PARC6, a novel chloroplast division factor, influences FtsZ assembly and is required for recruitment of PDV1 during chloroplast division in Arabidopsis. Plant J **59:** 700–711

Hale CA, de Boer PA (1997) Direct binding of FtsZ to ZipA, an essential component of the septal ring structure that mediates cell division in E. coli. Cell **88:** 175–185

Hu Z, Lutkenhaus J (1999) Topological regulation of cell division in Escherichia coli involves rapid pole to pole oscillation of the division inhibitor MinC under the control of MinD and MinE. Mol Microbiol **34:** 82–90

Hu Z, Mukherjee A, Pichoff S, Lutkenhaus J (1999) The MinC component of the division site selection system in Escherichia coli interacts with FtsZ to prevent polymerization. Proc Natl Acad Sci USA **96:** 14819–14824

Irieda H, Shiomi D (2017) ARC6-mediated Z ring-like structure formation of prokaryote-descended chloroplast FtsZ in Escherichia coli. Sci Rep-Uk **7**: 3492

Itoh R, Fujiwara M, Nagata N, Yoshida S (2001) A chloroplast protein homologous to the eubacterial topological specificity factor minE plays a role in chloroplast division. Plant Physiol **127:** 1644–1655

Li YQ, Sun QQ, Feng Y, Liu XM, Gao HB (2016) An improved immunofluorescence staining method for chloroplast proteins. Plant Cell Rep **35:** 2285–2293

Liu X, Gao Y, Shi Y, Shen X, Liu Z, Gao H (2012) Genetic mapping and analysis of a chloroplast division mutant cpd111 in Arabidopsis thaliana. Chin Bull Bot **47:** 226–235

Manna D, Bhardwaj N, Vora MS, Stahelin RV, Lu H, Cho W (2008) Differential roles of phosphatidylserine, PtdIns(4,5)P2, and PtdIns(3,4,5)P3 in plasma membrane targeting of C2 domains. Molecular dynamics simulation, membrane binding, and cell translocation studies of the PKCalpha C2 domain. J Biol Chem **283:** 26047–26058

Maple J, Vojta L, Soll J, Møller SG (2007) ARC3 is a stromal Z-ring accessory protein essential for plastid division. EMBO Rep **8:** 293–299

Mazouni K, Domain F, Cassier-Chauvat C, Chauvat F (2004) Molecular analysis of the key cytokinetic components of cyanobacteria: FtsZ, ZipN and MinCDE. Mol Microbiol **52:** 1145–1158

Miyagishima SY, Froehlich JE, Osteryoung KW (2006) PDV1 and PDV2 mediate recruitment of the dynamin-related protein ARC5 to the plastid division site. Plant Cell **18:** 2517–2530

Miyagishima SY, Nozaki H, Nishida K, Nishida K, Matsuzaki M, Kuroiwa T (2004) Two types of FtsZ proteins in mitochondria and red-lineage chloroplasts: the duplication of FtsZ is implicated in endosymbiosis. J Mol Evol **58:** 291–303

Nakanishi H, Suzuki K, Kabeya Y, Miyagishima S (2009) Plant-specific protein MCD1 determines the site of chloroplast division in concert with bacteria-derived MinD. Curr Biol **19:** 151–156

Olson BJSC, Wang QA, Osteryoung KW (2010) GTP-dependent heteropolymer formation and bundling of chloroplast FtsZ1 and FtsZ2. J Biol Chem **285:** 20634–20643

Osawa M, Anderson DE, Erickson HP (2008) Reconstitution of contractile FtsZ rings in liposomes. Science **320:** 792–794

Osteryoung KW, Vierling E (1995) Conserved cell and organelle division. Nature **376:** 473–474

Osteryoung KW, McAndrew RS (2001) The plastid division machine. Ann Rev Plant Physiol Plant Mol Biol **52:** 315–333

Osteryoung KW, Nunnari J (2003) The division of endosymbiotic organelles. Science **302:** 1698–1704

Osteryoung KW, Pyke KA (2014) Division and dynamic morphology of plastids. Annu Rev Plant Biol **65:** 443–472

Osteryoung KW, Stokes KD, Rutherford SM, Percival AL, Lee WY (1998) Chloroplast division in higher plants requires members of two functionally divergent gene families with homology to bacterial ftsZ. Plant Cell **10:** 1991–2004

Potocký M, Pleskot R, Pejchar P, Vitale N, Kost B, Zárský V (2014) Live-cell imaging of phosphatidic acid dynamics in pollen tubes visualized by Spo20p-derived biosensor. New Phytol **203:** 483–494

Resh MD (2016) Fatty acylation of proteins: the long and the short of it. Prog Lipid Res **63:** 120–131

Schmitz AJ, Glynn JM, Olson BJSC, Stokes KD, Osteryoung KW (2009) Arabidopsis FtsZ2-1 and FtsZ2-2 are functionally redundant, but FtsZ-based plastid division is not essential for chloroplast partitioning or plant growth and development. Mol Plant **2:** 1211–1222

Shaik RS, Sung MW, Vitha S, Holzenburg A (2018) Chloroplast division protein ARC3 acts on FtsZ2 by preventing filament bundling and enhancing GTPase activity. Biochem J **475:** 99–115

Simon ML, Platre MP, Marques-Bueno MM, Armengot L, Stanislas T, Bayle V, Caillaud MC, Jaillais Y (2016) A PtdIns(4)P-driven electrostatic field controls cell membrane identity and signalling in plants. Nat Plants **2:** 16089

Sreerama N, Woody RW (2000) Estimation of protein secondary structure from circular dichroism spectra: comparison of CONTIN, SELCON, and CDSSTR methods with an expanded reference set. Anal Biochem **287:** 252–260

Stokes KD, Osteryoung KW (2003) Early divergence of the FtsZ1 and FtsZ2 plastid division gene families in photosynthetic eukaryotes. Gene **320:** 97–108

Stokes KD, McAndrew RS, Figueroa R, Vitha S, Osteryoung KW (2000) Chloroplast division and morphology are differentially affected by overexpression of FtsZ1 and FtsZ2 genes in Arabidopsis. Plant Physiol **124:** 1668–1677

Szeto TH, Rowland SL, Rothfield LI, King GF (2002) Membrane localization of MinD is mediated by a C-terminal motif that is conserved across eubacteria, archaea, and chloroplasts. Proc Natl Acad Sci USA **99:** 15693–15698

TerBush AD, Porzondek CA, Osteryoung KW (2016) Functional analysis of the chloroplast division complex using Schizosaccharomyces pombe as a heterologous expression system. Microsc Microanal **22:** 275–289

Vitha S, McAndrew RS, Osteryoung KW (2001) FtsZ ring formation at the chloroplast division site in plants. J Cell Biol **153:** 111–120

Vitha S, Froehlich JE, Koksharova O, Pyke KA, van Erp H, Osteryoung KW (2003) ARC6 is a J-domain plastid division protein and an evolutionary descendant of the cyanobacterial cell division protein Ftn2. Plant Cell **15:** 1918–1933

Wang WH, Li JY, Sun QQ, Yu XY, Zhang WW, Jia N, An CJ, Li YQ, Dong YN, Han FJ, et al. (2017) Structural insights into the coordination of plastid division by the ARC6-PDV2 complex. Nat Plants **3**: 17011

Wang ZP, Xing HL, Dong L, Zhang HY, Han CY, Wang XC, Chen QJ (2015) Egg cell-specific promoter-controlled CRISPR/Cas9 efficiently generates homozygous mutants for multiple target genes in Arabidopsis in a single generation. Genome Biol **16:** 144

Xing HL, Dong L, Wang ZP, Zhang HY, Han CY, Liu B, Wang XC, Chen QJ (2014) A CRISPR/Cas9 toolkit for multiplex genome editing in plants. BMC Plant Biol **14:** 327

Yoshida Y, Mogi Y, TerBush AD, Osteryoung KW (2016) Chloroplast FtsZ assembles into a contractible ring via tubulin-like heteropolymerization. Nat Plants **2**: 16095

Zhang M, Schmitz AJ, Kadirjan-Kalbach DK, TerBush AD, Osteryoung KW (2013) Chloroplast division protein ARC3 regulates chloroplast FtsZ-ring assembly and positioning in Arabidopsis through interaction with FtsZ2. Plant Cell **25:** 1787–1802

Zhang M, Chen C, Froehlich JE, TerBush AD, Osteryoung KW (2016) Roles of Arabidopsis PARC6 in coordination of the chloroplast division complex and negative regulation of FtsZ assembly. Plant Physiol **170:** 250–262

Zhang M, Hu Y, Jia J, Li D, Zhang R, Gao H, He Y (2009) CDP1, a novel component of chloroplast division site positioning system in Arabidopsis. Cell Res **19:** 877–886